Diamond & Related Materials 96 (2019) 104–111

Contents lists available at ScienceDirect

Diamond & Related Materials

journal homepage: www.elsevier.com/locate/diamond

Influence of laser structuring and barium nitrate treatment on morphology and electrophysical characteristics of vertically aligned carbon nanotube arrays

Alexander Yu. Gerasimenko[a,d,*], Evgeny P. Kitsyuk[b], Artem V. Kuksin[a], Roman M. Ryazanov[b], Andrey I. Savitskiy[a,b], Mikhail S. Savelyev[a,d], Alexander A. Pavlov[c]

[a] National Research University of Electronic Technology MIET, bld. 1, Shokin Square, Zelenograd, Moscow 124498, Russia
[b] Scientific-Manufacturing Complex "Technological Centre", bld. 1-7, Shokin Square, Zelenograd, Moscow 124498, Russia
[c] Institute of Nanotechnology of Microelectronics of the Russian Academy of Sciences, Leninsky Prospekt 32A, Moscow 119991, Russia
[d] I.M. Sechenov First Moscow State Medical University, bld. 2-4, Bolshaya Pirogovskaya street, Moscow 119991, Russia

ARTICLE INFO

Keywords:
Carbon nanotube arrays
Vertically aligned
Laser irradiation
Structuring
Barium nitrate
Morphology
Nanosecond pulses
Modification
Electron field emission
Cathodes

ABSTRACT

The technology of structuring arrays of multilayer carbon nanotubes using pulsed laser radiation is presented. Arrays of two types nanotubes (long and short) with different morphologies were synthesized on a silicon substrate by the method of plasma enhanced chemical vapor deposition from the gas phase. Samples with arrays of nanotubes located strictly perpendicular to the silicon substrate were obtained using an ytterbium fiber laser (1064 nm) with a galvanometric scanner. Raman spectroscopy showed a decrease in the defectiveness of the carbon nanostructure of the tubes after laser irradiation. Liquid treatment with $Ba(NO_3)_2$ applied to the array with subsequent annealing resulted in sticking of the nanotubes at their tips. The formation of cellular structure from array of carbon nanotubes with a greater length after laser scanning of the sample was observed. Such arrays of nanotubes made it possible to increase the current of electron emission by more than two times at lower threshold voltage compared with the original arrays of nanotubes. The current density increased from 65 to 150 μA/cm^2. Structured arrays of nanotubes can be used to create efficient emission cathodes, as well as sensors, solar cells and MEMS structures.

1. Introduction

Currently, carbon nanotubes are widely used in science, medicine and industry. Nanotubes are promising materials for nanoelectronics. Due to the unique electrophysical properties, nanotubes are used as ultrasensitive active elements in functional devices. Large arrays of carbon nanotubes (CNT) can be used to create electron field emitters with non-standard shape [1]. The interest in field emission of cold cathodes is due to the low energy consumption and the small size of the emitter compared with thermal cathodes. The most promising materials for cold cathodes are carbon nanostructures, such as CNT [2,3]. One of the main advantages of emitters based on CNT arrays is the possibility of integrating the technology of their synthesis into the processes of microelectronic device creation. Such emitters have a low work function and high activation energy for the surface migration of atoms [4].

CNT arrays with given orientation are used to achieve effective field emission. Separate single CNT growing perpendicular to the substrate have different lengths, orientations, and shapes. There are a large number of chemical methods for the orientation of CNT arrays [5–7]. However, preference is given to optical methods that allow to change the structure and shape of CNT with a non-contact electromagnetic exposure [8–11]. In recent years, a large number of theoretical and experimental studies of the optical and nonlinear optical properties of carbon nanotubes have been carried out, which have proved the applicability of CNT in various optoelectronic devices [12–17].

Laser methods are widely used to produce micro and nanostructures in modern electronics, medicine, and industry [18–24]. The use of laser structuring of single-walled carbon nanotubes to create a carbon scaffold in biopolymer matrices at wavelengths of the short-wave infrared spectrum is known [25–27]. One of the first references to the use of the emitter, which is a laser-treated CNT array, is presented in [28–31]. The best emission current density values were obtained in places of laser radiation exposure on CNT lying on a glass substrate. The authors attribute this phenomenon to the rise of CNT lying on glass substrate

* Corresponding author at: National Research University of Electronic Technology MIET, Shokin Square, Zelenograd, Moscow 124498, Russia.
E-mail address: gerasimenko@bms.zone (A.Y. Gerasimenko).

https://doi.org/10.1016/j.diamond.2019.04.035
Received 11 December 2018; Received in revised form 27 March 2019; Accepted 29 April 2019
Available online 01 May 2019

Table 1
Parameters of CNT array synthesis.

Sample	Temperature, °C	Time, [min]	Pressure, [torr]	P, [W] (RF/LF)	Gas medium				
					C_2H_2, [cm^3/min]	Ar, [cm^3/min]	NH_3, [cm^3/min]	He, [cm^3/min]	H_2, [cm^3/min]
1	700	15	2	100/0	25	–	–	100	100
2	700	15	2	30/20	25	300	100	–	–

under the action of laser radiation. The most efficient alignment of the CNT array (the height of the structures formed is about 7.6 μm) was obtained using the third harmonic of the Nd:YAG laser (λ = 355 nm, τ = 10 ns, pulse fluence E/S = 326 mJ/cm^2) [32]. Laser-induced heating (λ = 266 nm, τ = 5 ns) of nickel oxide deposited on CNT arrays leads to the formation of the given nanotube morphology as a result of their cooling and crystallization [33]. This effect was achieved by the action of 100–2000 laser pulses, each of which had laser fluence of 40–260 mJ/cm^2.

Ordered CNT columns were created by the action of various lasers with wavelengths from 248, 355, 532, 1064, and 9300 nm, as well as nano- and picosecond pulse duration [34].

Irradiation of CNT arrays with a continuous laser at wavelength of 514 nm and radiation power of 70 mW made it possible to obtain emission current increase of 350 times, which corresponds to the current density of 0.13 A/cm^2. Laser irradiation of nanotubes decreases their defectiveness and increases resistance to high values of the electric field to 33 V/μm [35]. After CNT arrays irradiation with an excimer laser (λ = 308 nm), the emission current density value was reached up to 3.5 mA/cm^2, which corresponds to an increase of 100 times compared to the initial value before irradiation [36]. Laser deposition of carbon films with pulse fluence E/S = 20 J/cm^2 led to maximum current density of 1.6 mA/cm^2 at an average applied field of 4.6 V/mm [37]. Ethanol densified CNT films achieved consistent current density of 9–11 mA/cm^2 [38].

Also, irradiation with an excimer laser (λ = 248 nm, E/S = 150 mJ/cm^2) leads to an increase in the current density to 151 μA/cm^2 and a decrease in the exciting field to 2.61 V/μm [39]. With a decrease in the radiation energy density to 100 mJ/cm^2, the current density increased from 5.73 mA/cm^2 to 87.13 mA/cm^2, and the exciting field decreased from 3 V/μm to 2.1 V/μm [40].

The effect of CNT form on their emission characteristics was studied in [2]. Non-oriented, multidirectional nanotubes provide a maximum current density of 60 μA/cm^2. Rectified CNT with vertically directed ends allow to reach current density of 360 μA/cm^2, which corresponds to a six times increase. Under the influence of laser energy, it is possible to merge CNT into solid lines [36]. It was obtained that with the increase in length of the line by 7 times, the threshold voltage decreases by 1.4 times, which indicates an improvement in the electron emission characteristics.

Despite the achieved results in the field of creating cold cathodes based on structured CNTs, the requirements of modern technology are not satisfied. Since, to create structured CNT arrays on a substrate, complex technologies are used in conjunction with laser exposure, with the use of expensive materials: e-beam lithography, screen printing with indium tin oxide, etc. At the same time, the emission characteristics of grown CNT arrays are not always sufficient (low emission current density at its high voltage), and their sizes are limited by the creation technology. This paper presents simple and inexpensive technology of patterning multi-walled CNT array on silicon substrate under the action of pulsed laser radiation in the near-IR range. Based on the studies performed, a scalable technology for creating different size (from 1 μm to full substrate square) active elements of emitters with a given topology of multilayer carbon nanotube arrays was proposed.

2. Experiments and results

2.1. Synthesis of CNT arrays

CNT arrays were synthesized by the method of plasma enhanced chemical vapor deposition from the gas phase [41]. As the initial substrates, heavily doped single-crystal silicon wafers with electronic type conductivity were used. A catalytic pair of Ti (10 nm) and Ni (2 nm) was deposited on the substrate treated in a Piranha solution by electron beam evaporation. Next, the stages of oxidative and reductive annealing were carried out to form catalyst nanoparticles on the substrate.

For the synthesis of CNT, the Oxford PlasmaLab System 100 was used. Two different synthesis processes were carried out, which involved the creation of two CNT arrays with different morphology. The difference in the samples was determined by different parameters of the CNT synthesis (Table 1). The annealing parameters were identical for both samples: oxidation at 280 °C for 5 min. in O_2 and Ar with RF plasma of 100 W; recovery at 700 °C for 5 min in NH_3 and Ar with RF plasma of 100 W.

The average diameter of the CNTs in the arrays of two samples was determined mainly by the size of the formed catalyst nanoparticles on the substrate. The height of the CNT arrays of samples was very different. For sample 1, the height was ~8 μm, and for sample 2 it was ~4 μm (Fig. 1). On TEM images of CNT arrays, the structure of individual multilayer nanotubes can be seen (Fig.1e, f). The nanotubes of sample 1 had an outer diameter of 11–13 nm, the number of walls was 8–10, the wall thickness was 3.6–4.1 nm, and the diameter of the internal channel was 4.3–5.5 nm. The nanotubes of sample 2 had an outer diameter of 14–15 nm, the number of walls was 12–16, the wall thickness was 3.6–4.1 nm, and the diameter of the internal channel was 4.3–5.5 nm. The structure of the nanotubes of sample 1 was less defective and more perfect, as well as tubes were more smooth at the upper ends.

The alignment of nanotubes in the process of growing can be explained by the condensation effect from neighboring CNTs (crowding effect), that is, the holding of CNTs by means of van der Waals forces in an array with high density of nanotubes during their growth [42]. The CNT arrays of both samples look not quite straight, and the upper ends of the nanotubes are randomly directed (Fig. 1c, d). Such morphology of CNTs is not optimal for creating efficient electron emitters.

2.2. Laser structuring of CNT arrays

Pulsed laser radiation of ytterbium fiber laser with wavelength of 1064 nm, pulse duration of 100 ns, pulse repetition rate of 100 kHz was used to straighten CNTs over the entire area of the arrays. Average power was 0.7 W, which was measured by photodetector. The laser profile had Gaussian form. To arrange the laser beam in the point of sample, a galvanometric scanner with two mirrors was used (Fig. 2). The beam from the laser was transmitted via fiber to the scanner. Then the radiation fell on the lens, which focused the radiation on the sample surface. The lens had a focal length of 210 mm. The radiation was focused into a spot with a diameter of 35 μm. The laser pulse energy was 0.7 μJ, which was derived from the average power at the repetition rate up to 100 kHz. Thus, the fluence was ~1.5 J/cm^2 considering effective area of the beam. The optical setup was equipped with a distance sensor

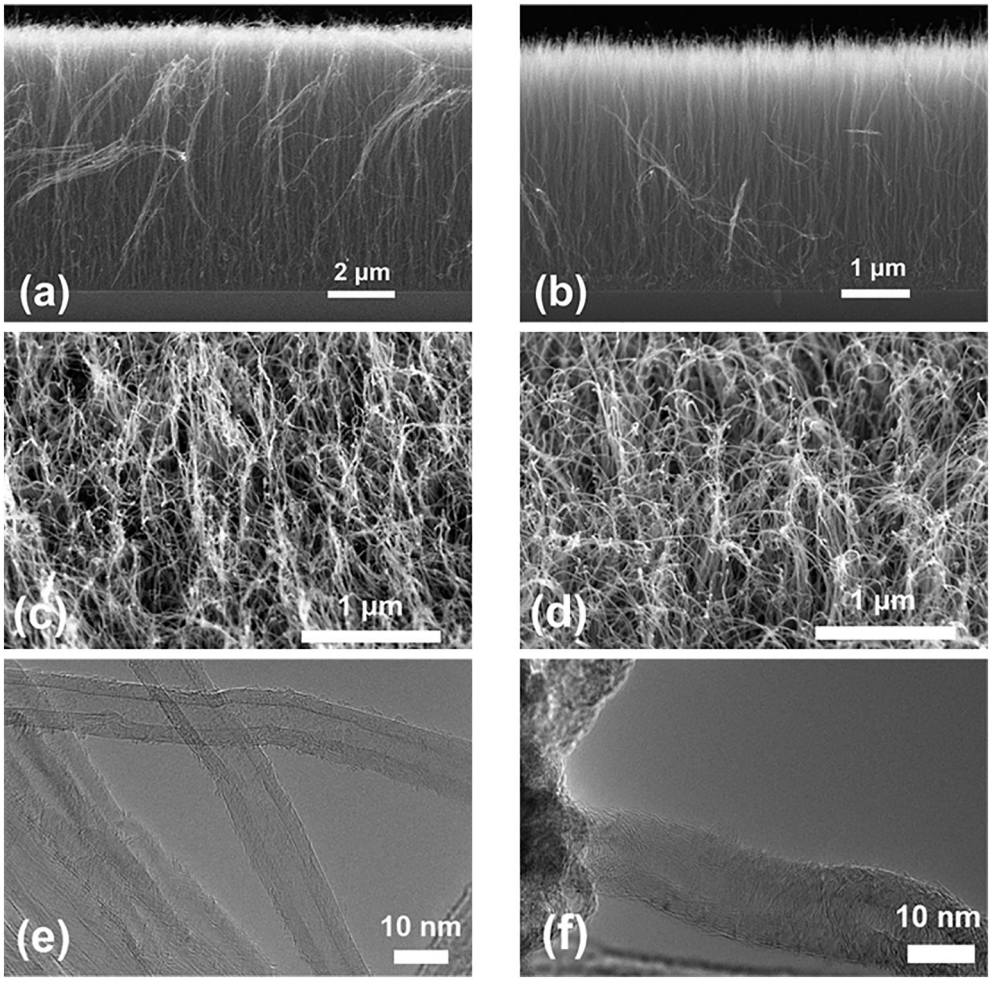

Fig. 1. SEM (a–d) and TEM (e, f) images of CNT arrays on silicon substrate with different magnification: (a, c, e) sample 1 (H_2 + He) and (b, d, f) sample 2 (Ar + NH_3).

for uniform irradiation of the sample area.

For laser processing of samples, the scanning parameters were set in specialized software. The speed of the beam movement along the path describing a square was 500 mm/s. When defining the irradiation trajectory, the option of filling the square with lines with a small overlap of laser spots was chosen. That was done to compensate the intensity of the Gaussian beam profile (Fig. 2). The lines of laser pulses were 5 mm long and were located parallel to each other at a distance of 17 μm. Thus, the structured areas of CNT arrays from 5 × 5 mm to 20 × 20 mm were formed.

For structuring of the sample 1 with a higher CNT array, a radiation power of 0.7 W was selected at fluence of ~1.5 J/cm^2. Fig. 3 shows the SEM images of a top view of the original and structured CNT arrays at the same scale and Raman spectra of CNT arrays. The perpendicular direction of the carbon nanotube ends relatively to the silicon substrate after the laser exposure is clearly visible.

The Raman spectra of the CNT arrays samples were obtained with Horiba LabRAM HR Evolution. The He-Ne laser (633 nm, 10 mW) was used as a source of excitation radiation. The diffraction grating 600 lines/mm provided the 1.5 cm^{-1} spectral resolution. The CCD

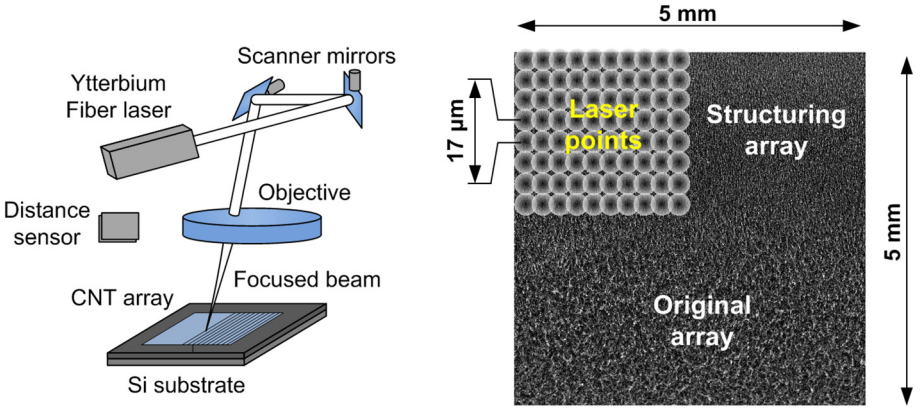

Fig. 2. Scheme of the optical setup and laser points on the CNT array.

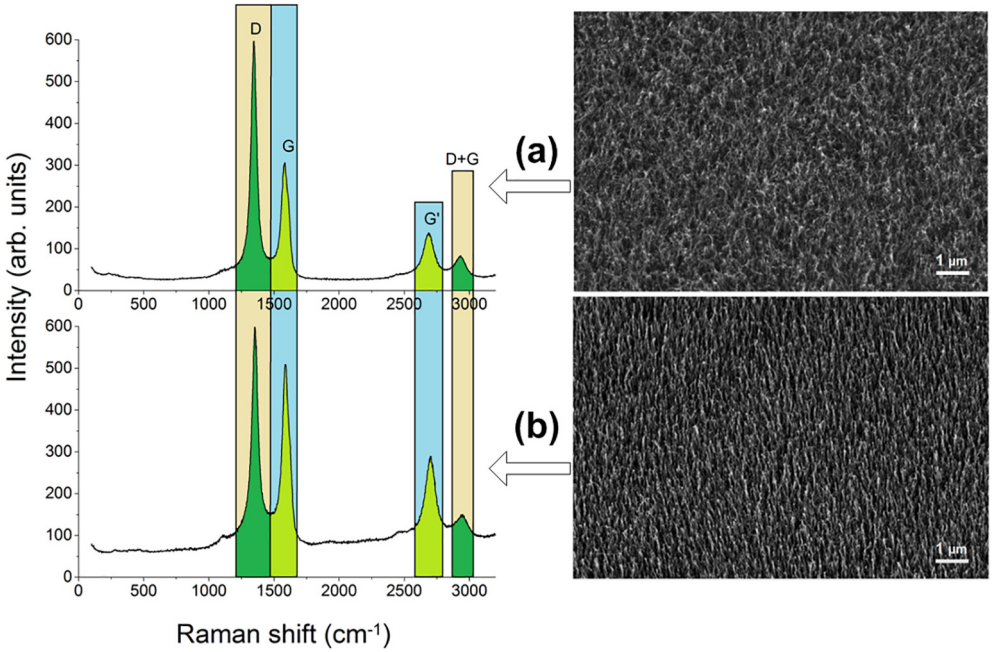

Fig. 3. Raman spectra and SEM images of CNT arrays in sample 1: (a) original and (b) laser-structured.

camera was cooled at 200 K for detecting Stokes-side Raman scattering at a wide spectral range. The precision motorized stage and on-board Olympus BX41 microscope were used for the laser beam focusing on the investigated area. The accumulation time and accumulation number were 10 s and 4 s, respectively. The calibration of the LabRAM HR spectrometer was verified before and after each investigated sample by acquiring Raman spectra of a standard silicon wafer.

2.3. Formation of complex structures from CNT arrays

It is known that the work function of material critically affects its emission characteristics. For carbon nanotubes, electron emission values of 4.8–5.0 eV are generally accepted [43]. The search for methods for reducing the work function during electron emission led to the idea of CNT array treatment with barium-based substances. Such substances are widely used for thermionic cathodes. By the experimental method, the most effective composition for processing the CNT arrays with $Ba(NO_3)_2$ was selected.

Since nanotubes exhibit hydrophobic properties immediately after synthesis, the method of plasma CNT array treatment was used to impart hydrophilic properties to them. For this purpose, the treatment process was carried out in an $Ar + O_2$ gas mixture at working pressure in the chamber of 5.24 Pa. The processing time was 30 s and the plasma power was 30 W.

The samples 1 and 2 with CNT arrays area of 1 cm^2 were uniformly applied with a liquid composition of barium nitrate $Ba(NO_3)_2$ with volume of 20 μl at concentration 0.03 mg/ml. From thermogravimetric analysis of $Ba(NO_3)_2$, it was determined that $Ba(NO_3)_2$ decomposes to nitrite $Ba(NO_2)_2$ at ~400 °C and to BaO oxide at 700 °C. The CNTs were vacuum-annealed at a temperature of 800 °C for 15 min. It was found, that effect of BaO on samples 1 and 2 leads to sticking of the nanotubes at their upper ends. At the same time, there is formation of islands from stuck nanotubes. The CNT array structures of the samples 1 and 2 were significantly different. CNT synthesized in H_2 and He medium (sample 1), shown in Fig. 4.

Next, the CNT arrays were scanned by laser radiation with the parameters presented in the previous section of the article. The inner part and the contours of the cells were completely made of nanotubes (Fig. 5c). In the center of the cells, the nanotubes looked more

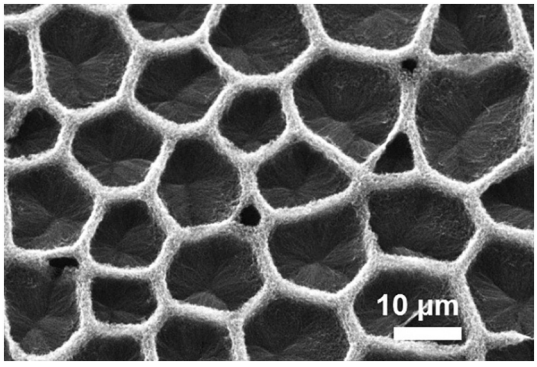

Fig. 4. SEM image of structured CNT arrays using $Ba(NO_3)_2$ treatment of sample 1.

straightened comparatively to the original array. The cells basically had 5–7 vertices each. The cell size in sample 1 was 5–70 μm (Fig. 5a). Thus, nanotubes under the action of BaO interlaced into separate structures. After that, they were separated and shortened under the action of pulsed laser radiation, and they were vertically oriented perpendicular to the substrate (Fig. 5c, d). Part of the sublimated carbon and BaO particles were deposited on the upper ends of the nanotubes after laser irradiation. This can be seen in Fig. 5e, f for both arrays. Presumably, mainly amorphous carbon is subjected to sublimation. Arrays of short CNTs synthesized in NH_3 and Ar (sample 2) showed more resistance to laser irradiation (Fig. 5a). In this case, only sticking of closely located CNT occurred. CNT arrays took the form of cells with fuzzy boundaries. The cell size was 1–10 μm. High magnification images show that the tips of the tubes at the edges of the cells were connected (Fig. 5c, f). Also, the tips of the tubes were coated with particles of sublimated carbon and BaO after laser treatment. The adhesion of nanotubes and the mixing of their structure at the ends is shown in TEM for both arrays (Fig. 5g, h).

Most likely, the effect of CNT structuring by liquid annealing and laser irradiation depends on the length of the nanotubes in array. Another important factor while laser structuring is the morphology of the array. The CNT arrays synthesized in the NH_3-Ar medium, did not made it possible to obtain cells with clear boundaries at any length of

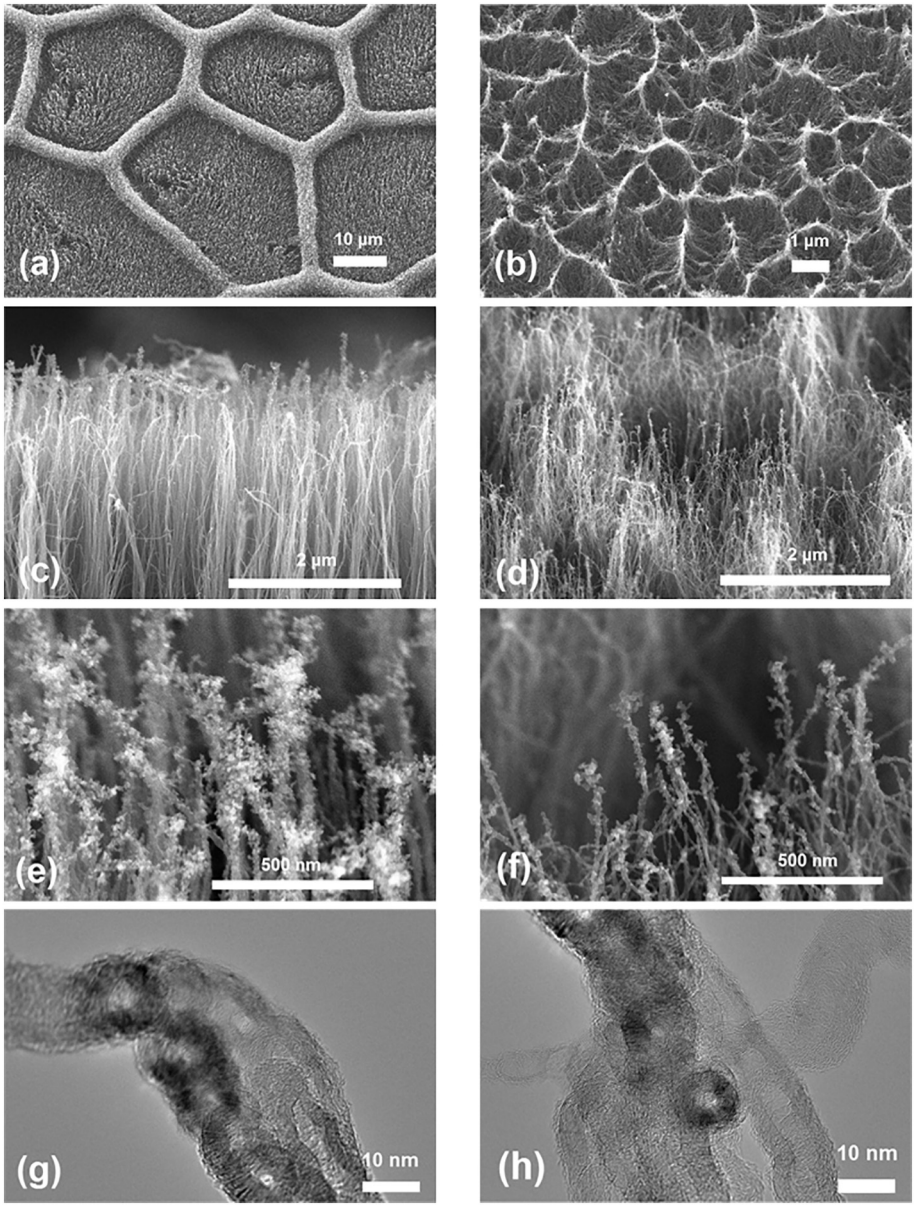

Fig. 5. SEM (a–f) and TEM (g, h) images of structured CNT arrays using $Ba(NO_3)_2$ treatment and laser irradiation with different magnification: sample 1 (a, c, e, g) and sample 2 (b, d, f, h).

the nanotubes.

The energy-dispersive X-ray spectroscopy (EDX) was used to determine the chemical composition of the created nanostructure. EDX map of barium distribution over the surface of the treated array is shown in Fig. 6c. For identification of the studied area, a SEM image is shown and a map of carbon distribution in the same area is shown for comparison (Fig. 6a, b). It can be seen that the barium covered the almost entire study area of the treated array.

2.4. Electrophysical characteristics of CNT arrays

The field electron emission characteristics of the samples were studied at intermediate and final stages of CNT array processing. Measurement of the current-voltage characteristics of the samples was carried out using a vacuum chamber, to which the forevacuum and high-vacuum cryogenic pumps supporting pressure were connected (Fig. 7). The sample was fixed on a ceramic table, the first electrode (cathode) was connected to it. The table was equipped with heating elements and a thermocouple, which allowed to set and maintain temperature. The second electrode (anode) with a rounded tip was fed from above to the substrate with CNT arrays at distance of 3 μm. The anode was moved along the XYZ axes using stepper motors with accuracy of 10 nm. Such system made it possible to create a potential difference between the anode and the cathode in DC mode from 0 to 1000 V. For measurements of the electrical characteristics, a programmable dual-channel source-meter SourceMeter 2410C Keithley was used.

Measurement of the electron emission of the CNT arrays after exposure to only BaO showed a change in the current-voltage characteristics for both samples as compared to the original array (Fig. 8). Sample 1 showed an increase in current, but its threshold voltage was not changed. The original array of sample 2 showed the greatest current at the highest voltage. But the effect of BaO on it led to strong deterioration of the current while maintaining the threshold voltage at the same level. The effect of BaO on CNT arrays does not always lead to an improvement in the field electron emission characteristics of the array. Largely, they are determined by the characteristics of the array. Despite the similar exterior of the original arrays, their characteristics are

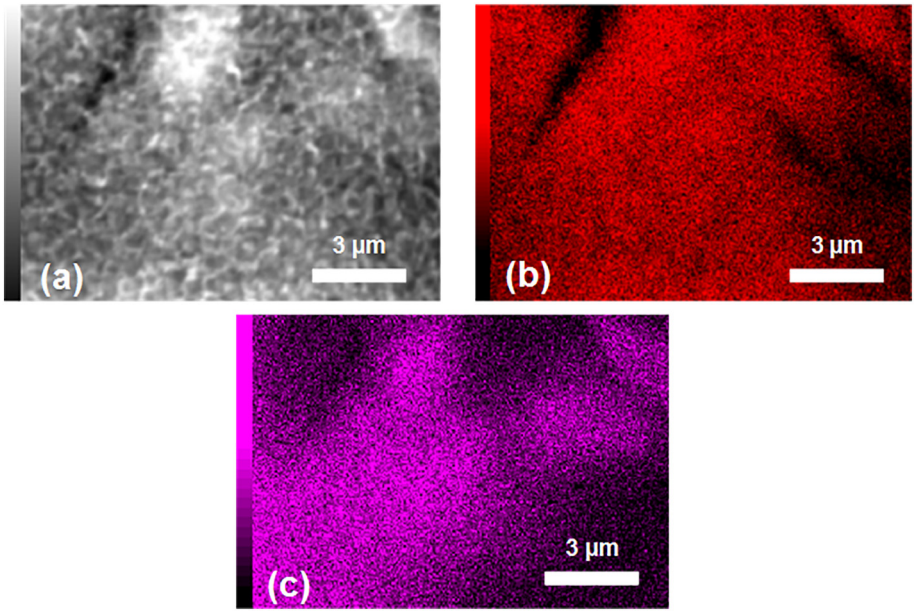

Fig. 6. SEM image of structured CNT arrays using $Ba(NO_3)_2$ treatment and laser irradiation (a), carbon (b) and barium EDX mapping (c).

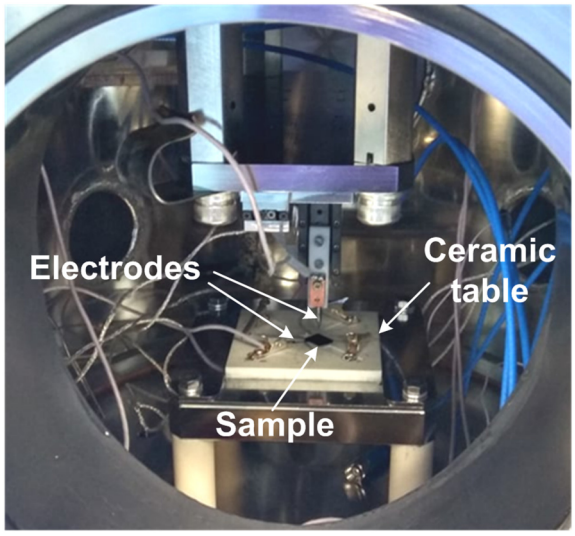

Fig. 7. Setup for measuring the electron emission of CNT arrays.

radically different, even without the effect of BaO. The effect can both improve and degrade the parameters of CNT array, and it can only be determined experimentally.

Fig. 8 shows the current-voltage characteristics after laser structuring. The structured CNT array of sample 1 provided an increase in current and a slight decrease in threshold voltage, compared with the original array and BaO-treated nanotubes. However, the CNT array processing of sample 2 does not bear positive changes in emission characteristics. When the current decreases, the threshold voltage increases, which indicates deterioration in the characteristics of the sample.

3. Discussion

Thus, this paper presents the results of structuring the synthesized CNT arrays. Two types of samples were studied that differed in the length of nanotubes with almost the same diameter. Sample 1 synthesized in the H_2 + He gas environment had length of nanotubes in the array twice as large (~8 μm) as compared to the array of sample 2 (4 μm), which was synthesized in the Ar + NH_3 gas mixture. When laser pulses of ytterbium laser (λ = 1064 nm) were impacted on long and short CNT arrays, the effect of structuring nanotubes perpendicular to the silicon substrate was obtained. This effect can be caused by change in the defectiveness of the carbon nanostructure of the tubes. The expansion of air due to heating generates a stream directed perpendicularly from the substrate to the ends of the nanotubes. Such flow can straighten nanotubes. After cooling, the position of the tubes is fixed. At the same time, the degree of imperfection of carbon nanotubes in the long and short arrays significantly decreases. When nanotubes are heated by laser pulses with duration of 100 ns, the defective areas will be

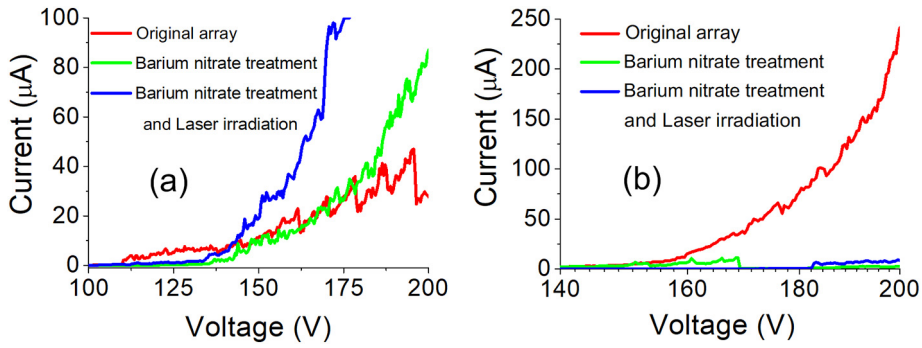

Fig. 8. Current-voltage characteristics of the original CNT arrays, after its processing with BaO and after laser structuring: (a) of sample 1 and (b) of sample 2.

heated most strongly, since the thermal conductivity in these areas is much lower [25]. The heated defect areas of the nanotubes become more chemically active and able to form bonds. Therefore, in Fig. 3b, single nanotubes closely spaced to each other are sticking closer to their tops.

In the course of growing nanotubes array, it is difficult to obtain a homogeneous holistic structure for the entire array and individual tubes as a whole, since there is a high probability that bends/curvatures or lattice defects will appear depending on the preparation method. Raman spectroscopy is an excellent tool for detecting this kind of structural defects. In particular, it allows estimating the degree of defectiveness after structuring. It has been established that CNT defectiveness. The Raman spectra of obtained samples include the characteristic scattering bands G and D, G′ and a D + G. When bonds are broken in the structure, atoms with sp3-hybridized electrons appear outside the plane of the nanotube layers. In this case, the atoms oscillate with the frequency of the D mode, and not of the G mode, therefore, its intensity decreases with a strong defectiveness. The intensity ratio of the D/G modes for a structured array is much lower compared to the original CNT array. At the same time, the peaks ~1350 cm^{-1} intensity decreases slightly after laser structuring, which indicates that the selected fluence of laser irradiation does not damage the main number of CNTs. The position of G mode is characteristic of MWCNTs and is located near 1585 cm^{-1}.

The ratio of the D and G band intensity (I_D/I_G) is often used in the analysis of the defectiveness of graphite and graphite-like materials [44]. Experiments have shown that the initially grown nanotubes have the value of I_D/I_G = 1.95, which indicates a high density of nanotube defects on the dome-shaped tips or side “wavy” nanotube surfaces. After laser structuring, the ratio I_D/I_G = 1.18, which may be associated with the formation of new compounds at the points of breaking the carbon atom bonds, as well as the sublimation of amorphous carbon. The aspiration of this value to 1 indicates a more graphitized sample structure. G′ band, located ~2695 cm^{-1} corresponds to the overtone of the D band and characterizes the degree of “purity” of the sample, since it cannot be caused by structural defects, [45] and the peak ~2940 cm^{-1} belongs to second-order Raman modes D + G [46]. An increase in the intensity of the G′ mode in conjunction with a change in the intensity ratio I_D/I_G confirms the process of structuring the MWCNT samples.

To form complex structures from CNT arrays, a method of connecting nanotubes into bundles using high-temperature annealing (800 °C) in the presence of $Ba(NO_3)_2$ was applied. At the same time, a cellular structure was formed with the upper ends of the nanotubes stuck together. After laser treatment of the long CNT array, mainly cells with pentagonal, hexagonal and heptagonal structure were formed. The structure of such array resembled Rayleigh-Benard convective cells [47]. As a result of pulsed laser irradiation, the nanotubes of sample 1 were separated and straightened perpendicular to the substrate. The short array of sample 2 almost after similar laser treatment visually remained in its original state (except for the upper ends).

The method of synthesis of CNT chemical vapor deposition from the gas phase favorably differs from other methods by its low cost, and the emission characteristics of the resulting arrays are not inferior to those obtained by other authors, and sometimes even exceed them [35,38]. This conclusion is confirmed by measuring the emission characteristics. The emission characteristics of the short CNT array became worse after the patterning of BaO nanotubes and laser radiation. Most likely, this is due to the deterioration of the aspect ratio of the CNT array. Sample 1 showed opposite results. The temperature structuring of the long array treated with BaO led to a significant increase in current from 47 to 88 μA at voltage of 200 V. The laser structuring effect increased current of the CNT array in cells to 100 μA at voltage of 175 V. Current density increased from 65 to 150 mA/cm^2. At the same voltage for the original array and the CNT array after BaO processing, current was ~30 μA. Thus, during laser structuring of the long CNT array into cells, the shape of a sharply increasing curve is obtained in Fig. 8a. It is obtained that a high value of current is achieved at a reduced voltage values. Thus, we propose a new method for improving emission characteristics by structuring the CNT array with barium nitrate treatment and laser scanning. This technology allows creating a structured CNT arrays with a large area. The technology is scalable and can be used to create active elements of emitters with a given topology of multilayer arrays of carbon nanotubes with various sizes (from 1 μm to the total area of the substrate).

4. Conclusion

The result of this work is the optical technology of new nanostructures formation to create efficient emission cathodes, which can be widely used in scientific research, medical equipment, industrial complexes, etc. The technology of laser CNT array patterning can be used to create new sensitive elements of photodetectors, solar batteries, chemical sensors, temperature and pressure sensors, microscopy probes, MEMS structures etc.

Two types of CNT arrays with different length were synthesized by catalytic PECVD method. CNT arrays were vertically aligned to their tips using the pulsed laser. Cellular structure of CNT array was created using barium nitrate treatment and laser irradiation. The morphology of the CNT arrays was investigated using electron microscopy. Structure synthesized with H_2 and He has shown increased field emission.

Acknowledgements

This study was supported by the Russian Science Foundation, project no. 18-79-10008 and Russian Academic Excellence Project “5–100” for Sechenov First Moscow State Medical University. The studies were performed using MIET Core facilities center “MEMS and electronic components”.

References

[1] G. Bocharov, A. Eletskii, Theory of carbon nanotube (CNT)-based electron field emitters, Nanomaterials 3 (2013) 393–442, https://doi.org/10.3390/nano3030393.
[2] F. Le Normand, C.S. Cojocaru, C. Fleaca, J.Q. Li, P. Vincent, G. Pirio, L. Gangloff, Y. Nedellec, P. Legagneux, A comparative study of the field emission properties of aligned carbon nanostructures films, from carbon nanotubes to diamond, Eur. Phys. J. Appl. Phys. 38 (2007) 115–127, https://doi.org/10.1051/epjap:2007052.
[3] X. Yuan, M. Cole, Y. Zhang, J. Wu, W. Milne, Y. Yan, Parametrically optimized carbon nanotube-coated cold cathode Spindt arrays, Nanomaterials 7 (2017) 13, https://doi.org/10.3390/nano7010013.
[4] W. Hoenlein, F. Kreupl, G.S. Duesberg, A.P. Graham, M. Liebau, R. Seidel, E. Unger, Carbon nanotubes for microelectronics: status and future prospects, Mater. Sci. Eng. C. 23 (2003) 663–669, https://doi.org/10.1016/j.msec.2003.09.153.
[5] H. Xin, A.T. Woolley, Directional orientation of carbon nanotubes on surfaces using a gas flow cell, Nano Lett. 4 (2004) 1481–1484, https://doi.org/10.1021/nl049192c.
[6] T. Vad, J. Wulfhorst, T.-T. Pan, W. Steinmann, S. Dabringhaus, M. Beckers, G. Seide, T. Gries, W.F.C. Sager, M. Heidelmann, T.E. Weirich, Orientation of well-dispersed multiwalled carbon nanotubes in melt-spun polymer fibers and its impact on the formation of the semicrystalline polymer structure: a combined wide-angle X-ray scattering and electron tomography study, Macromolecules 46 (2013) 5604–5613, https://doi.org/10.1021/ma4001226.
[7] U. Suryavanshi, A.V. Baskar, V.V. Balasubramanian, S.S. Al-Deyab, A. Al-Enizi, A. Vinu, Growth and physico-chemical properties of interconnected carbon nanotubes in FeSBA-15 mesoporous molecular sieves, Arab. J. Chem. 9 (2016) 171–178, https://doi.org/10.1016/j.arabjc.2015.04.024.
[8] H. Xin, B. Li, Optical orientation and shifting of a single multiwalled carbon nanotube, Light Sci. Appl. 3 (2014) e205, https://doi.org/10.1038/lsa.2014.86.
[9] B.H. Lee, J.W. Cho, K.H. Kim, Crystallization, orientation, and mechanical properties of laser-heated photothermally drawn polypropylene/multi-walled carbon nanotube fibers, Eur. Polym. J. 91 (2017) 70–80, https://doi.org/10.1016/j.eurpolymj.2017.03.051.
[10] J.W. Hur, H.J. Yoo, J.W. Cho, K.H. Kim, Orientation and mechanical properties of laser-induced photothermally drawn fibers composed of multiwalled carbon nanotubes and poly(ethylene terephthalate), J. Polym. Sci. Part B Polym. Phys. 54 (2016) 603–609, https://doi.org/10.1002/polb.23953.
[11] M. Spellauge, F.-C. Loghin, J. Sotrop, M. Domke, M. Bobinger, A. Abdellah, M. Becherer, P. Lugli, H.P. Huber, Ultra-short-pulse laser ablation and modification of fully sprayed single walled carbon nanotube networks, Carbon N. Y. 138 (2018)

234–242, https://doi.org/10.1016/j.carbon.2018.05.074.
[12] S.A. Tereshchenko, M.S. Savelyev, V.M. Podgaetsky, A.Y. Gerasimenko, S.V. Selishchev, Nonlinear threshold effect in the Z-scan method of characterizing limiters for high-intensity laser light, J. Appl. Phys. 120 (2016) 093109, , https://doi.org/10.1063/1.4962199.
[13] S. Siregar, S. Oktamuliani, Y. Saijo, A theoretical model of laser heating carbon nanotubes, Nanomaterials 8 (2018) 580, https://doi.org/10.3390/nano8080580.
[14] M. Chernysheva, A. Rozhin, Y. Fedotov, C. Mou, R. Arif, S.M. Kobtsev, E.M. Dianov, S.K. Turitsyn, Carbon nanotubes for ultrafast fibre lasers, Nanophotonics. 6 (2017) 1–30, https://doi.org/10.1515/nanoph-2015-0156.
[15] H.H. Van, K. Badura, M. Zhang, Laser-induced transformation of freestanding carbon nanotubes into graphene nanoribbons, RSC Adv. 5 (2015) 44183–44191, https://doi.org/10.1039/C5RA05836H.
[16] M. Siciński, E. Korzeniewska, M. Tomczyk, R. Pawlak, D. Bieliński, T. Gozdek, K. Kałuzińska, M. Walczak, Laser-textured rubbers with carbon nanotube fillers, Polymers (Basel) 10 (2018) 1091, https://doi.org/10.3390/polym10101091.
[17] E. György, Á. Pérez del Pino, J. Roqueta, B. Ballesteros, L. Cabana, G. Tobias, Effect of laser radiation on multi-wall carbon nanotubes: study of shell structure and immobilization process, J. Nanopart. Res. 15 (2013) 1852, , https://doi.org/10.1007/s11051-013-1852-6.
[18] J. Koch, Direct-write subwavelength structuring with femtosecond laser pulses, Opt. Eng. 44 (2005) 051103, , https://doi.org/10.1117/1.1904053.
[19] M. De Feudis, A.P. Caricato, A. Taurino, P.M. Ossi, C. Castiglioni, L. Brambilla, G. Maruccio, A.G. Monteduro, E. Broitman, G. Chiodini, M. Martino, Diamond graphitization by laser-writing for all-carbon detector applications, Diam. Relat. Mater. 75 (2017) 25–33, https://doi.org/10.1016/j.diamond.2016.12.019.
[20] L. Jonušauskas, S. Rekštytė, R. Buividas, S. Butkus, R. Gadonas, S. Juodkazis, M. Malinauskas, Hybrid subtractive-additive-welding microfabrication for lab-on-chip applications via single amplified femtosecond laser source, Opt. Eng. 56 (2017) 1, https://doi.org/10.1117/1.OE.56.9.094108.
[21] V.Y. Iakovlev, Y.A. Sklyueva, F.S. Fedorov, D.P. Rupasov, V.A. Kondrashov, A.K. Grebenko, K.G. Mikheev, F.Z. Gilmutdinov, A.S. Anisimov, G.M. Mikheev, A.G. Nasibulin, Improvement of optoelectronic properties of single-walled carbon nanotube films by laser treatment, Diam. Relat. Mater. 88 (2018) 144–150, https://doi.org/10.1016/j.diamond.2018.07.006.
[22] D.T.T. Nguyen, O. Del Guercio, T.H. Au, D.T. Trinh, N.P.T. Mai, N.D. Lai, Optical lithography of three-dimensional magnetophotonic microdevices, Opt. Eng. 57 (2018) 1, https://doi.org/10.1117/1.OE.57.4.041406.
[23] A.V. Kabashin, P. Delaporte, A. Pereira, D. Grojo, R. Torres, T. Sarnet, M. Sentis, Nanofabrication with pulsed lasers, Nanoscale Res. Lett. 5 (2010) 454–463, https://doi.org/10.1007/s11671-010-9543-z.
[24] Q. Li, D. Grojo, A.-P. Alloncle, B. Chichkov, P. Delaporte, Digital laser micro- and nanoprinting, Nanophotonics 8 (2018) 27–44, https://doi.org/10.1515/nanoph-2018-0103.
[25] A.Y. Gerasimenko, O.E. Glukhova, G.V. Savostyanov, V.M. Podgaetsky, Laser structuring of carbon nanotubes in the albumin matrix for the creation of composite biostructures, J. Biomed. Opt. 22 (2017) 065003, , https://doi.org/10.1117/1.JBO.22.6.065003.
[26] I.B. Rimshan, N.N. Zhurbina, U.E. Kurilova, D.I. Ryabkin, A.Y. Gerasimenko, Biocompatible nanomaterial for restoration of continuity of dissected biological tissues, Biomed. Eng. (NY). 52 (2018) 23–26, https://doi.org/10.1007/s10527-018-9774-3.
[27] L.P. Ichkitidze, V.M. Podgaetsky, S.V. Selishchev, A.A. Dudin, A.A. Pavlov, Electrical Conductivity of the Nanocomposite Layers for in Biomedical Systems, vol. 37, (2018), pp. 140–145.
[28] J.I. Sohn, S. Lee, Y.-H. Song, S.-Y. Choi, K.-I. Cho, K.-S. Nam, Large field emission current density from well-aligned carbon nanotube field emitter arrays, Curr. Appl. Phys. 1 (2001) 61–65, https://doi.org/10.1016/S1567-1739(00)00012-2.
[29] J.I. Sohn, C. Nam, S. Lee, Vertically aligned carbon nanotube growth by pulsed laser deposition and thermal chemical vapor deposition methods, Appl. Surf. Sci. 197–198 (2002) 568–573, https://doi.org/10.1016/S0169-4332(02)00338-0.
[30] R. Angelucci, R. Rizzoli, S. Salvatori, S. Nicoletti, A. Migliori, E. Brugnoli, Amorphous carbon deposited by pulsed laser ablation as material for cold cathode flat emitters, Appl. Surf. Sci. 186 (2002) 423–428, https://doi.org/10.1016/S0169-4332(01)00711-5.
[31] F.C. Cheong, K.Y. Lim, C.H. Sow, J. Lin, C.K. Ong, Large area patterned arrays of aligned carbon nanotubes via laser trimming, Nanotechnology 14 (2003) 433–437, https://doi.org/10.1088/0957-4484/14/4/305.
[32] A. Lasagni, R. Cross, S. Graham, S. Das, The fabrication of high aspect ratio carbon nanotube arrays by direct laser interference patterning, Nanotechnology 20 (2009) 245305, , https://doi.org/10.1088/0957-4484/20/24/245305.
[33] A. Pérez del Pino, E. Gyorgy, S. Hussain, J.L. Andújar, E. Pascual, R. Amade, E. Bertrán, Laser-induced nanostructuration of vertically aligned carbon nanotubes coated with nickel oxide nanoparticles, J. Mater. Sci. 52 (2017) 4002–4015, https://doi.org/10.1007/s10853-016-0662-5.
[34] J.W. Elmer, O. Yaglioglu, R.D. Schaeffer, G. Kardos, O. Derkach, Direct patterning of vertically aligned carbon nanotube arrays to 20 μm pitch using focused laser beam micromachining, Carbon N. Y. 50 (2012) 4114–4122, https://doi.org/10.1016/j.carbon.2012.04.059.
[35] G. Ulisse, F. Brunetti, A. Di Carlo, S. Orlanducci, E. Tamburri, V. Guglielmotti, M. Marrani, M.L. Terranova, Carbon nanotubes field emission enhancement using a laser post treatment, J. Vac. Sci. Technol. B, Nanotechnol. Microelectron. Mater. Process. Meas. Phenom. 33 (2015) 022203, , https://doi.org/10.1116/1.4913285.
[36] A. Hosono, T. Shiroishi, K. Nishimura, F. Abe, Z. Shen, S. Nakata, S. Okuda, Emission characteristics of printed carbon nanotube cathodes after laser treatment, J. Vac. Sci. Technol. B Microelectron. Nanom. Struct. 24 (2006) 1423, https://doi.org/10.1116/1.2202123.
[37] H. Jadhav, A.K. Singh, S. Sinha, Pulsed laser deposition of graphite in air and in vacuum for field emission studies, Mater. Chem. Phys. 162 (2015) 279–285, https://doi.org/10.1016/j.matchemphys.2015.05.068.
[38] Y.D. Lim, Q. Kong, S. Wang, C.W. Tan, B.K. Tay, S. Aditya, Enhanced field emission properties of carbon nanotube films using densification technique, Appl. Surf. Sci. 477 (2019) 211–219, https://doi.org/10.1016/j.apsusc.2017.11.005.
[39] C.-W. Cheng, C.-M. Chen, Y.-C. Lee, Laser surface treatment of screen-printed carbon nanotube emitters for enhanced field emission, Appl. Surf. Sci. 255 (2009) 5770–5774, https://doi.org/10.1016/j.apsusc.2009.01.005.
[40] K.-J. Chen, W.-K. Hong, C.-P. Lin, K.-H. Chen, L.-C. Chen, H.-C. Cheng, Improvement of field emission characteristics of carbon nanotubes by excimer laser treatment, Jpn. J. Appl. Phys. 41 (2002) 6132–6136, https://doi.org/10.1143/JJAP.41.6132.
[41] M. Meyyappan, L. Delzeit, A. Cassell, D. Hash, Carbon nanotube growth by PECVD: a review, Plasma Sources Sci. Technol. 12 (2003) 205–216, https://doi.org/10.1088/0963-0252/12/2/312.
[42] S. Fan, Self-oriented regular arrays of carbon nanotubes and their field emission properties, Science 80 (283) (1999) 512–514, https://doi.org/10.1126/science.283.5401.512.
[43] W.S. Su, T.C. Leung, C.T. Chan, Work function of single-walled and multiwalled carbon nanotubes: first-principles study, Phys. Rev. B 76 (2007) 235413, , https://doi.org/10.1103/PhysRevB.76.235413.
[44] S.C. Ramos, G. Vasconcelos, E.F. Antunes, A.O. Lobo, V.J. Trava-Airoldi, E.J. Corat, Wettability control on vertically-aligned multi-walled carbon nanotube surfaces with oxygen pulsed DC plasma and CO_2 laser treatments, Diam. Relat. Mater. 19 (2010) 752–755, https://doi.org/10.1016/j.diamond.2010.01.044.
[45] M.S. Dresselhaus, G. Dresselhaus, R. Saito, A. Jorio, Raman spectroscopy of carbon nanotubes, Phys. Rep. 409 (2005) 47–99, https://doi.org/10.1016/j.physrep.2004.10.006.
[46] P. Tan, S. Dimovski, Y. Gogotsi, Raman scattering of non–planar graphite: arched edges, polyhedral crystals, whiskers and cones, Philos. Trans. R. Soc. London. Ser. A Math. Phys. Eng. Sci. 362 (2004) 2289–2310, https://doi.org/10.1098/rsta.2004.1442.
[47] M. Assenheimer, V. Steinberg, Rayleigh-Bénard convection near the gas-liquid critical point, Phys. Rev. Lett. 70 (1993) 3888–3891, https://doi.org/10.1103/PhysRevLett.70.3888.